Published in final edited form as:
J Neurosci. 2009 October 7; 29(40): 12521–12531. doi:10.1523/JNEUROSCI.0640-09.2009.

Gamma-band Synchronization in the Macaque Hippocampus and Memory Formation

Michael J. Jutras[1,2], **Pascal Fries**[3,4], and **Elizabeth A. Buffalo**[1,2,5]

[1] Yerkes National Primate Research Center, Atlanta, GA, 30329 [2] Neuroscience Program, Emory University, Atlanta, GA, 30329 [3] Donders Institute for Brain, Cognition and Behaviour, Radboud University Nijmegen, Nijmegen, The Netherlands [4] Ernst-Strüngmann-Institute in Cooperation with the Max-Planck-Society, Frankfurt, Germany [5] Department of Neurology, Emory University School of Medicine, Atlanta, GA, 30329

Abstract

Increasing evidence suggests that neuronal synchronization in the gamma band (30–100 Hz) may play an important role in mediating cognitive processes. Gamma-band synchronization provides for the optimal temporal relationship between two signals to produce the long-term synaptic changes that have been theorized to underlie memory formation. While neuronal populations in the hippocampus oscillate in the gamma range, the role of these oscillations in memory formation is still unclear. In order to address this issue, we recorded neuronal activity in the hippocampus while macaque monkeys performed a visual recognition memory task. During the encoding phase of this task, hippocampal neurons displayed gamma-band synchronization. Additionally, enhanced gamma-band synchronization during encoding predicted greater subsequent recognition memory performance. These changes in synchronization reflect enhanced coordination among hippocampal neurons and may facilitate synaptic changes necessary for successful memory encoding.

Keywords

hippocampus; memory; gamma; oscillation; synchronization; coherence

Introduction

Accumulating evidence suggests that along with changes in the firing rates of individual neurons, the precise timing of neuronal activity may play an important role in cognition. Synchronization of neuronal activity in the gamma-frequency band (30 to 100 Hz) has been related to selective attention (Fries et al., 2001; Bichot et al., 2005; Taylor et al., 2005; Womelsdorf et al., 2006; Buschman and Miller, 2007; Fries et al., 2008) and working memory (Pesaran et al., 2002). Additionally, studies of intracranial electroencephalography in epilepsy patients suggest that gamma-band synchronization may be an important component in successful memory encoding (Fell et al., 2001; Sederberg et al., 2007b). By aligning periods of inhibition, gamma-band synchronization establishes precise coordination in the spike times of neurons responding to behaviorally relevant stimuli (Mishra et al., 2006; Womelsdorf et al., 2007). Gamma-band synchronization among a group of neurons ensures that presynaptic spikes

Address for correspondence: Elizabeth Buffalo, Yerkes National Primate Research Center, 954 Gatewood Road, Atlanta, GA, 30329, elizabeth.buffalo@emory.edu.
Senior Editor: Earl Miller

arrive at mutual downstream targets within ~10 ms of each other. Since mutual synaptic input is followed reliably by postsynaptic spikes, this precise temporal relationship provides the necessary conditions for long term changes in synaptic strength, which is considered to be one of the primary information storage principles in the brain (Markram et al., 1997; Bi and Poo, 1998). However, to date, there has been little direct evidence for a relationship between gamma-band synchronization among hippocampal neurons and memory formation.

Recognition memory, the ability to perceive a recently encountered item as familiar, is degraded following damage to the hippocampus in humans and monkeys (Zola et al., 2000; Manns et al., 2003), although findings regarding the role of the hippocampus in recognition memory have not always been consistent across laboratories (Murray and Mishkin, 1998; Baxter and Murray, 2001a, b; Zola and Squire, 2001; Nemanic et al., 2004). To add to this controversy, only a very small number of neurons have been reported to display recognition memory signals in the hippocampus proper (Brown et al., 1987; Rolls et al., 1989; Riches et al., 1991; Rolls et al., 1993; Xiang and Brown, 1998; but see Rutishauser et al., 2006). The apparent inconsistency between the findings from lesion and physiology studies raises doubt about the contribution of the hippocampus to recognition memory.

All of these previous neurophysiological studies examined changes in firing rate that might act as a signal for recognition memory. However, it is possible that recognition signals in the hippocampus may take the form of enhanced neuronal synchronization among groups of neurons. Here, we examined the relationship between neuronal synchronization among hippocampal neurons and recognition memory performance on the Visual Preferential Looking Task in monkeys. This task has been shown to depend upon the integrity of the hippocampus in both monkeys (Pascalis and Bachevalier, 1999; Zola et al., 2000; Nemanic et al., 2004) and humans (McKee and Squire, 1993). We report that hippocampal neurons show gamma-band synchronization during encoding that is positively correlated with subsequent recognition memory performance. These changes in synchronization reflect enhanced interaction among hippocampal neurons and may provide a mechanism for the synaptic changes necessary for successful memory formation.

Materials and Methods

Procedures were carried out in accordance with NIH guidelines and were approved by the Emory University Institutional Animal Care and Use Committee. Neuronal recordings were made in two adult male rhesus monkeys (*Macaca mulatta*), obtained from the breeding colony at the Yerkes National Primate Research Center. Their mean weight at the start of the experiment was 6.8 ± 1.1 kg, and their mean age was 4 years and 5 months. Prior to implantation of recording hardware, monkeys were scanned with magnetic resonance imaging (MRI) to localize the hippocampus and to guide placement of the recording chamber. Using this information, a cilux plastic chamber (Crist Instrument Co., Hagerstown, MD) for recording neural activity, and a titanium post for holding the head were surgically implanted. Post-surgical MRI was performed to localize recording sites.

Behavioral testing procedures

During testing, each monkey sat in a dimly illuminated room, 60 cm from a 19 inch CRT monitor that had a resolution of 800 × 600 pixels and a screen refresh rate of 120 Hz noninterlaced. Eye movements were recorded using a non-invasive infrared eye-tracking system (ISCAN, Burlington, Massachusetts).

Stimuli were presented using experimental control software (CORTEX, www.cortex.salk.edu). At the beginning of each recording session, the monkey performed an

eye-position calibration task, which involved holding a touch-sensitive bar while fixating a small (0.3°) gray fixation point, presented on a dark background at various locations on the monitor. The monkey was required to maintain fixation within a 3° window until the fixation point changed to an equiluminant yellow at a randomly chosen time between 500 ms and 1100 ms after fixation onset. The monkey was required to release the touch sensitive bar within 500 ms of the color change for delivery of a drop of applesauce. During this task, the gain and offset of the oculomotor signals were adjusted so that the computed eye position matched targets that were a known distance from the central fixation point.

Visual Preferential Looking Task

Following the calibration task, the monkey was tested on the Visual Preferential Looking Task (VPLT; Figure 1A). The monkey initiated each trial by fixating a white cross (1°) at the center of the computer screen. After maintaining fixation on the cross for 1 s, the cross disappeared and the picture stimulus (11°) was presented. The stimulus disappeared when the monkey's direction of gaze moved off the stimulus, or after a maximum looking time of 5 s. Each trial was followed by a 1 s intertrial interval. The VPLT was given in 51 daily blocks of 6, 8, or 10 trials each, chosen pseudorandomly, for a total of 400 trials each day. Each session, monkeys were presented with a total of 200 unique, complex stimuli. Each stimulus was presented twice during a given session, with up to 8 intervening stimuli between successive presentations. A total of 9000 stimuli were used in this study.

Because the monkey controlled the duration of stimulus presentation, the duration of gaze on each stimulus provides a measure of the monkey's preference for the stimulus. We compared the amount of time the monkey spent looking at each stimulus during its first and second presentation. We designated the novel presentation of each stimulus the "encoding" phase and the repeated presentation the "recognition" phase of the task. Adult monkeys show a strong preference for novelty; therefore, a significant reduction in looking time between the two presentations of a stimulus indicated that the monkey had formed a memory of the stimulus and spent less time looking at the now familiar stimulus during its second presentation (Wilson and Goldman-Rakic, 1994). To control for varying interest in individual stimuli, recognition memory performance was calculated as the absolute change in looking time between presentations as a percentage of the amount of time the monkey spent looking at the first presentation of each stimulus.

Reward was not delivered during VPLT trials. However, 5 trials of the calibration task were presented between each VPLT block in order to give the monkey a chance to earn some reward and to verify calibration of the eye position. The number of trials in each VPLT block was varied to prevent the monkey from knowing when to expect the rewarded calibration trials.

Electrophysiological recording methods

The recording apparatus consisted of a multi-channel microdrive (FHC Inc., Bowdoinham, Maine) holding a manifold consisting of a single 23-gauge guide tube containing 4 independently moveable tungsten microelectrodes (FHC Inc., Bowdoinham, Maine), with each electrode inside an individual polyamide tube. Electrode impedance was in the range of 1–2 MΩ, and electrode tips were separated horizontally by 190 μm. For each recording, the guide tube was slowly lowered through the intact dura mater and advanced to ~3.5 mm dorsal to the hippocampus with the use of coordinates derived from the MRI scans. The electrodes were then slowly advanced out of the guide tube to the hippocampus. No attempt was made to select neurons based on firing pattern. At the end of each recording session, the microelectrodes and guide tube were retracted. All recordings took place in the anterior part of the left hippocampus.

Recording sites were located in the CA3 field, dentate gyrus, and subiculum (see Supplemental Figure 1).

Data amplification, filtering, and acquisition were performed with a Multichannel Acquisition Processor (MAP) system from Plexon Inc. (Dallas, TX). The neural signal was split to separately extract the spike and the LFP components. For spike recordings, the signals were filtered from 250 Hz – 8 kHz, further amplified and digitized at 40 kHz. A threshold was set interactively, in order to separate spikes from noise, and spike waveforms were stored in a time window from 150 μs before to 700 μs after threshold crossing. Each recording typically yielded 2 to 6 units; single units were sorted offline using Offline Sorter (Plexon, Inc.). For LFP recordings, the signals were filtered with a passband of 0.7–170 Hz, further amplified and digitized at 1 kHz. Eye movement data were digitized and stored with a 240 Hz resolution.

Data Analysis

All analyses were performed using custom programming in Matlab (The Mathworks, Inc., Natick, MA) and using FieldTrip (http://www.ru.nl/fcdonders/fieldtrip/), an open source Matlab toolbox. To ensure that the monkeys had sufficient time to perceive the stimuli, analyses were limited to pairs of trials (corresponding to the two presentations of each stimulus) in which monkeys examined stimuli for at least 750 ms during the first presentation, which resulted in an average of 135 pairs of trials per session.

For each neuron, firing rate was calculated for the period including pre-stimulus fixation as well as stimulus presentation. Significant responses to stimuli were determined using a Student's t-test to compare activity for the period from 100–500 ms after stimulus onset to a baseline period of 300 ms preceding stimulus onset. Only neurons judged to be visually responsive, i.e., those which displayed a significant mean firing rate modulation upon the first (encoding) presentation, were included in further analyses.

For the calculation of coherence and power spectra, the multi-taper method was used in order to achieve optimal spectral concentration (Mitra and Pesaran, 1999; Jarvis and Mitra, 2001; Pesaran et al., 2002; Womelsdorf et al., 2006). Multitaper methods involve the use of multiple data tapers for spectral estimation. A 250 ms segment of data was multiplied by a data taper before Fourier transformation. A variety of tapers can be used, but an optimal family of orthogonal tapers is given by the prolate spheroidal functions or Slepian functions. For time length T and bandwidth frequency W, up to K=2TW-1 tapers are concentrated in frequency and suitable for use in spectral estimation. We used three Slepian tapers, providing an effective taper smoothing of ±8 Hz. For each taper, the data segment was multiplied with that taper and Fourier transformed, giving the windowed Fourier transform, $\tilde{x}_k(f)$:

$$\tilde{x}_k(f) = \sum_{1}^{N} w_k(t) x_t e^{-2\pi i f t}$$

where x_t, (t= 1,2,…, N) is the time series of the signal under consideration and $w_k(t)$, (k= 1,2, …, K) are K orthogonal taper functions. For spike signals, the firing rate was represented with a bin width of one millisecond and then subjected to spectral analysis like LFPs.

The multitaper estimates for the spectrum $S_x(f)$ and the cross-spectrum $S_{yx}(f)$ are given by

$$S_x(f)=\frac{1}{K}\sum_{1}^{K}|\tilde{x}_k(f)|^2$$

$$S_{yx}(f)=\frac{1}{K}\sum_{1}^{K}\tilde{y}_k(f)\tilde{x}_k^*(f)$$

Spectra and cross-spectra are averaged over trials before calculating the coherency C_{yx} (f)

$$C_{yx}(f)=\frac{S_{yx}(f)}{\sqrt{S_x(f)S_y(f)}}$$

Coherency is a complex quantity. Its absolute value is termed coherence and ranges from 0 to 1. A coherence value of 1 indicates that the two signals have a constant phase relationship (and amplitude covariation), a value of 0 indicates the absence of any phase relationship. Thus, coherence is a measure of linear predictability that captures phase and amplitude correlations.

Coherence spectra were calculated between the spiking activity obtained on one electrode and LFP activity derived from a different electrode. Both coherence and power analyses were limited to LFPs derived from electrodes that also had isolated single units in order to ensure that LFPs were obtained from cell layers. We did not calculate coherence between LFPs and spiking activity obtained on the same electrode. This gave us a maximum of 3 spike-LFP coherence spectra for each neuron. Spike-spike coherence spectra were also calculated between visually-responsive neurons recorded within the same recording session, using the same methods described above for the calculation of coherence spectra between spiking activity and LFP activity.

Correlating neuronal activity with memory performance

Two methods were used to determine the relationship between neuronal activity and subsequent recognition memory performance. First, neuronal activity during encoding was compared for the stimuli that evoked the best and worst memory. The stimuli from each session were ranked in order of increasing recognition performance, quantified as the percent change in looking time between first and second presentations for each stimulus. The 30 encoding trials with the lowest percent change were designated “Low Recognition” and the 30 trials with the highest percent change were designated “High Recognition”. After removing trials for which the looking time during the first stimulus presentation was 750 ms or less, 30 trials represented a median of 22.2% of all trials in the session. Comparisons between the two stimulus groups were made for neuronal firing rates, the evoked LFP response, spike and LFP power, spike-field coherence (SFC), and spike-spike coherence (SSC).

Neuronal Firing Rate

Each neuron’s visual response magnitude was calculated across both groups of 30 trials from 100–500 ms after stimulus onset, expressed as a percentage of the baseline firing rate (such that a decrease in firing rate at stimulus onset assumed a negative value, and an increase in firing rate assumed a positive value). The absolute value of each neuron’s percent change value was used to enable grouping of neurons with enhanced and depressed responses in the same analysis. Finally, a Student’s t-test was used to determine whether the magnitude of the visual response was significantly different for High and Low Recognition trials across the population.

Evoked LFP

To compare stimulus-evoked LFPs across the two conditions, we calculated an average LFP across all LFPs time-locked to stimulus onset, for High Recognition and Low Recognition trials. We then divided these signals into 10 ms bins and, using a Student's t-test, obtained a p-value for each bin. This allowed us to determine time points at which the two signals diverged significantly.

Spike and LFP Spectra

Power spectra were calculated for each spike signal and all LFPs derived from electrodes that also had isolated single units, using the multi-taper method (see details above). For spike spectra, neurons with enhanced firing rate responses to stimulus onset were analyzed separately from neurons with depressed firing rate responses. Correlations between spectra and recognition memory were tested using a nonparametric permutation test (see details below).

Spike-Field Coherence

In order to compare the average SFC across all neuron-LFP pairs during encoding of High Recognition and Low Recognition conditions, the frequency range within the 30–100 Hz gamma-band for which each neuron-LFP pair showed the highest SFC at 100–400 ms after stimulus onset across all encoding trials was identified (average frequency window size was 21.4 ± 0.7 Hz). SFC was calculated within this frequency window across all High Recognition and Low Recognition trials, separately for each pair. Then, these values were averaged across all neuron-LFP pairs.

To test for statistical significance of differences between spectra during the High Recognition and Low Recognition conditions, we performed a nonparametric permutation test, with the median difference between conditions as our test statistic. The test involves a comparison of the observed difference against a reference distribution of differences under the null hypothesis of no significant modulation of the spike or LFP power or SFC at individual frequencies between conditions. The reference distribution was obtained by performing the following procedure 10,000 times. For each recording site (or pairs of sites), a random decision was made to which condition the data from either condition was assigned. We then calculated the test statistic at each frequency for these randomly assigned conditions and stored only the minimal and maximal difference across frequencies. From the resulting distribution of 10,000 minimal and maximal differences, we determined the 2.5th and the 97.5th percentile. The empirically observed, nonrandomized difference at a particular frequency was considered statistically significant ($p < 0.05$), when it was larger than the 97.5th or smaller than the 2.5th percentile of the reference distribution. This procedure corresponds to a two-sided test with a global false positive rate of 5% and correction for the multiple comparisons across frequencies (Nichols and Holmes, 2002; Maris and Oostenveld, 2007). We used this non-parametric permutation approach, because 1) it is free of assumptions about the underlying distributions 2) it is not affected by partial dependence among the time-frequency tiles 3) it allows for correction for multiple comparisons without additional assumptions.

Additionally, we identified neuron-LFP pairs showing significant gamma-band coherence using the following method. To test the significance of coherence values, we calculated the time-averaged coherence across the time period of 100–400 ms after stimulus onset for each pair, then transformed these values to Z-scores using the following formula:

$$Z=\text{arctanh}(\sqrt{C}) \times \sqrt{2L}$$

where C is the coherence value and L is the number of independent estimates (Rosenberg et al., 1989; Kilner et al., 2000). Z-transformed coherence values were thus calculated for each neuron-lfp pair, across all high recognition trials (novel presentations of the 30 stimuli from each session for which the monkey subsequently showed the best recognition). We considered a pair to have significant spike-field coherence if this Z-transformed gamma-band coherence value was greater than 2 for at least 5 consecutive frequency values (spanning 16.6 Hz).

Spike-spike Coherence

Our methods for analyzing the relationship between SSC for visually-responsive neuron pairs and behavior are identical to the analyses applied to SFC data, as described above. Specifically, the Z-transformed coherence values were used to determine neuron-neuron pairs with significant gamma-band coherence, and the nonparametric permutation test described above was used to determine whether spike-spike coherence was significantly correlated with memory performance.

Correlations with Memory and Attention: Binning Analysis

The second analysis we performed to determine the relationship between neuronal activity and performance considered correlations on a trial-by-trial basis. For each recording session, encoding trials were sorted in two ways: in terms of increasing percent change in looking time between the encoding trial and the subsequent repetition of the stimulus (recognition memory performance), and in terms of total looking time for the encoding trial (attention). For each measure, 10 bins of 30 trials each were defined, with bin centers spaced at equivalent intervals. An equal number of trials per bin was used to avoid sample size biases. As a consequence, in some cases, this resulted in slightly overlapping bins and a few trials that were not included in any bin. For each neuron-LFP pair, the frequency range for which the pair showed the highest SFC at 100–400 ms after stimulus onset across all encoding trials was identified, and then the SFC in that frequency range at 100–400 ms was calculated, separately for each bin, across the 30 trials in each bin. Finally, the correlation between the 10 bins of each task parameter value (either recognition memory performance or attention) and coherence during encoding was calculated. Across pairs of recording sites, this resulted in a population of correlation coefficients and slopes for each measure. A sign test was performed on each distribution to determine statistical significance.

For the stimulus-evoked LFP, this analysis was performed in the way described above with one difference: for each bin of trials, we averaged the LFP amplitude from 270–570 ms after stimulus onset for novel trials (the time during which there was a significant difference in the LFP amplitude between High Recognition and Low Recognition trials across all recorded LFPs). The slope and the correlation coefficient were calculated for this trial-averaged LFP amplitude across all bins, separately for each LFP. A sign test was then performed on each distribution of slopes and correlation coefficients.

Correlations with Time within Session: Binning Analysis

In order to determine possible changes in behavior or neuronal activity that may have occurred within the session, for each recording session, all 200 stimuli were organized into the order in which they were presented within each session. Ten bins of 20 stimuli each were then defined, and five measures were calculated for each bin: the mean percent change in looking time from the first to the second presentation (recognition memory performance); the absolute looking time during novel stimulus presentation; the firing rate modulation, defined as the absolute value of the change in firing rate from the 300 ms preceding stimulus onset to the time period 100–500 ms after stimulus onset; gamma-band SFC from 100–400 ms after stimulus onset, using the same frequency window as that used in the binning analysis described above; and

LFP amplitude averaged over the time period of 270–570 ms after stimulus onset for each novel stimulus presentation.

Results

Behavioral Results

Figure 1B depicts an example of the monkey's eye movements during the first (yellow trace) and second (red trace) presentations of a stimulus in the VPLT. In this example, and across the majority of trials, the monkey spent more time looking at a stimulus when it was novel compared to when it was repeated. Across 45 sessions, the monkeys demonstrated robust recognition memory performance. There was a significant ($p < 0.001$) decrease in looking time for the repeated presentation (average looking times for Novel and Repeat trials were 2.7 s and 0.8 s, respectively). The median reduction in looking time was 70.7% (67.3% in Monkey A and 72.8% in Monkey B) (Figure 1C).

Neuronal Activity in the Hippocampus

We recorded spikes from 131 isolated single neurons (67 in Monkey A and 64 in Monkey B, respectively) as well as local field potentials (LFPs) in the hippocampal formation in two rhesus monkeys performing the VPLT. Eighty-six neurons (66%) gave a significant response to the first (encoding) presentation of stimuli, with either enhanced (34 neurons) or depressed (52 neurons) responses as compared to baseline (Figure 2A; Supplemental Table 1). Consistent with recent findings from human epilepsy patients (Rutishauser et al., 2006), a substantial proportion of these visually-responsive units (36%) showed a modulation in firing rate based on stimulus novelty.

Neuronal synchronization during the encoding phase of the task was assessed by calculating SFC between each visually-responsive neuron and the LFP recorded simultaneously on a separate electrode ($n = 175$ neuron-LFP pairs). The LFP results from the extracellular current flow that corresponds primarily to the summed postsynaptic potentials from the dendritic fields of local cell groups (Buzsaki, 2004). Thus, SFC is a measure of linear predictability that captures phase and amplitude correlations between neuronal input (LFP) and output (spiking activity). SFC typically increased upon visual stimulation, and these increases were most prominent in the 1–8 Hz range (delta/theta-band), and the 30–100 Hz range (gamma-band). Coherence below 20 Hz was not significantly modulated by recognition memory performance on the VPLT. Accordingly, we have confined our analysis and discussion to neuronal synchronization in the gamma band.

Across the population gamma-band SFC tended to cluster in one of two frequency bands: low gamma (30–60 Hz, Figures 2B and 2C, bottom) and high gamma (60–100 Hz, Figure 2B and 2C, top). Out of 86 neurons, 42 displayed a range of coherence which included coherence in the 60 Hz band. However, not all those neurons necessarily showed coherence centered around 60 Hz: 20 neurons displayed a band of increased coherence with 60 Hz as either the upper or lower limit, and thus had a substantial portion of increased coherence either above or below 60 Hz. Of the remaining 22 neurons, only 4 showed peak coherence at 60 Hz. For these neurons, we designated each as high or low gamma based on the entire frequency band in which the neuron showed coherence during encoding trials, and whether the bulk of this frequency band lay above or below 60 Hz. Using this method, 3 neurons were designated as high gamma and 1 was designated as low gamma. There was no significant relationship between the peak frequency of gamma-band coherence and the response properties of neurons: 59% of neurons with enhanced firing responses to stimuli exhibited coherence in the low gamma range, while 56% of neurons with depressed firing responses to stimuli exhibited coherence in high gamma ($p > 0.10$; Supplemental Table 1).

We additionally analyzed all neuron-LFP pairs with visually responsive single units to determine how many pairs exhibited significant SFC during the initial presentation of subsequently well-recognized stimuli. Out of these neuron-LFP pairs, 151 (86%) met the criterion we set for significant gamma-band SFC. Additionally, out of 83 pairs of simultaneously recorded visually-responsive neurons, 54 pairs (65%) showed significant gamma-band SSC during high recognition trials.

Hippocampal Gamma-band Synchronization Reflects Recognition Memory Performance

Figures 3A and 3B depict the firing rate and SFC for High Recognition and Low Recognition trials for an example recording pair. For this example neuron, and across the population, firing rates during encoding were not significantly modulated by subsequent recognition memory performance ($p > 0.05$; Figure 3A). By contrast, for this example (Figure 3B) and across the population (Figure 3, C–F), gamma-band coherence was enhanced during the encoding of stimuli that were subsequently well recognized relative to those stimuli that were poorly recognized.

Increases in SFC during the presentation of novel stimuli usually covered limited frequency bands within the broader gamma-band range. This tendency of spikes to lock coherently with LFPs in a narrow band of a particular gamma frequency has also been reported in the rodent neocortex (Sirota et al., 2008). For this reason, we identified a separate frequency range for each neuron in order to analyze changes in SFC with respect to memory (see Materials and Methods). Figure 3C shows the average recognition-related modulations in coherence across the population of recording sites. “High Recognition” represents the gamma-band SFC during the encoding of the 30 stimuli in each session with the best subsequent recognition, and “Low Recognition” corresponds to the 30 stimuli with the worst recognition. Across the population, there was an approximately 10% increase in gamma-band synchronization during encoding of stimuli that were subsequently well recognized relative to those stimuli that were poorly recognized. This enhancement reached significance beginning 120 ms after stimulus onset.

Average SFC for the two memory conditions are displayed separately for spike-field pairs displaying high- (above 60 Hz peak frequency, Figure 3D) and low-gamma synchronization (below 60 Hz, Figure 3E; see online Supplemental Methods for details). The results of the non-parametric permutation analysis revealed that gamma-band coherence was significantly enhanced during high recognition trials as early as 100 ms after stimulus onset for high-gamma spike-field pairs ($p < 0.05$, corrected for multiple comparisons; Figure 3F, top panel). Although there was a strong trend for enhanced gamma-band coherence across the low gamma spike-field pairs, this did not reach statistical significance (Figure 3F, bottom panel). This may have been due to a lack of sensitivity because the same analysis using multi-unit activity revealed significant memory-related modulations in gamma-band coherence for both high-gamma and low-gamma pairs (see Supplemental Figure 2). Because the sensitivity of coherence measures are proportional to the number of neurons contributing to the analysis, coherence analyses of single unit activity are less sensitive than analyses of multi-unit activity (Zeitler et al., 2006). Therefore, it is possible that single unit spike-field coherence did not reach significance for the Low Gamma group because of a loss in sensitivity compared to the multi-unit analysis.

We also tested whether spike-spike coherence (SSC) was significantly correlated with memory performance using the non-parametric permutation test. Each neuron-neuron pair showing significant coherence was designated as “high gamma” or “low gamma” based on the frequency band in which coherence across all novel stimulus presentations increased in the time period of 100–400 ms after stimulus onset. We applied the permutation test to each group of pairs separately: a small, but significant, cluster of spike-spike coherence (SSC) was seen for the high gamma pairs ($n = 32$) but not for the low gamma pairs ($n = 22$). This result is presented in the Supplemental Material (Supplemental Figure 3).

Relationship between Gamma-band Synchronization and Behavior: Memory vs. Attention

It is important to consider whether the observed synchronization among hippocampal neurons primarily reflects successful memory encoding or the attentive state of the animal. Increased attention to a stimulus likely leads to more successful memory encoding and may cause enhanced neuronal synchronization among hippocampal neurons. With 200 novel stimuli in each recording session, we have to assume that some stimuli are more interesting to the monkey and attract the monkey's attention more than other stimuli. Because the task design allows the monkey to determine the length of stimulus presentation by continuing to look at or looking away from each stimulus, we take as an assumption that the length of looking time for the initial presentation of a stimulus (encoding) reflects the animal's interest in, and attention to, the stimulus. Although other factors may influence looking time in isolated instances, e.g. the monkey's distractibility, over many trials, the monkey's interest in and attention to the stimulus is most likely the overriding factor in determining looking time during novel presentation. If hippocampal synchronization reflects primarily attentive mechanisms, increasing gamma-band coherence in the hippocampus would correlate with increasing length of time spent looking at novel stimuli. To quantify the extent to which neuronal synchronization among hippocampal neurons correlated with recognition memory and attention, for each recording session, we organized all encoding trials into bins, either by increasing recognition memory performance (expressed as the percent change in looking time) or increased attention (expressed as the duration of looking time during the encoding phase). We then correlated the magnitude of spike-field coherence and the behavioral measures of recognition memory performance and attention, as described in Materials and Methods. For the example neuron-LFP pair depicted in Figure 4A, gamma-band spike-field coherence was significantly correlated with recognition memory performance ($p < 0.005$; Figure 4A, left) but not with attention ($p > 0.10$; Figure 4A, right). Across the population, the correlation coefficients and the slopes for all neuron-LFP pairs displayed a significant positive distribution ($p < 0.001$; Figures 4B and 4C, left) for recognition memory performance, but not for attention ($p > 0.10$; Figures 4B and 4C, right). A consistent result was obtained when the multiple spike-field coherence results for each single unit were averaged (Supplemental Figure 4). These data suggest that the attentive state of the animal during encoding, as indexed by duration of looking, does not explain the effects of hippocampal gamma-band synchronization on recognition memory performance.

Previous studies have found that principal cells and interneurons play different roles in the generation of gamma-band oscillations in the hippocampus (Bragin et al., 1995; Chrobak and Buzsaki, 1996; Csicsvari et al., 2003). We categorized neurons as putative principal cells or putative interneurons, taking into consideration both the average firing rate during the fixation period preceding stimulus onset and the width of spike waveforms. Both populations of neurons displayed significant gamma-band spike-field coherence modulations during stimulus encoding that predicted subsequent recognition memory (data not shown). Of the 76 visually-responsive putative pyramidal cells, 39 were classified as "high gamma" and 37 as "low gamma". Ten neurons were classified as putative interneurons, 4 of which were designated "high gamma". Accordingly, the data do not suggest that the high vs. low gamma classification was correlated with cell type.

Along with coherence, we also derived power spectra for all LFPs and spike trains. There was no significant effect of memory performance on power in the spike spectra across the population (data not shown). However, LFP power from 40–65 Hz was significantly enhanced during the encoding of well-remembered stimuli compared with the encoding of poorly remembered stimuli approximately 80–300 ms after stimulus onset (Figure 5). Although the gamma-band power effects occurred at the same time as the effects in gamma-band coherence, it is important to note that spike-field coherence is normalized by power in both the spike

spectrum and the LFP spectrum (see Methods). In other words, coherence represents the consistency of the phase relation between the single unit rhythm and the LFP rhythm, irrespective of the power in either rhythm. Thus, although both signals are correlated with the strength of memory encoding, each represents a distinct neural mechanism.

The results from the non-parametric permutation test revealed significant differences between memory conditions for spike-field coherence, spike-spike coherence, and gamma-band power after stimulus onset. However, there were also small clusters of increased gamma-band coherence against background activity prior to stimulus onset (Figures 3D and 3E). An additional permutation test applied to the baseline period prior to stimulus onset revealed no clusters of significant pre-stimulus modulations for either single-unit SFC (Supplemental Figure 5), multi-unit SFC (Supplemental Figure 2A), single-unit SSC (Supplemental Figure 3A), or gamma-band power (Supplemental Figure 6). Therefore, unlike the stimulus-related activity, none of the pre-stimulus activity we recorded was modulated by recognition memory performance.

Relationship between Local Field Potential and Behavior

There have been a number of studies investigating neural activity during presentation of novel or rare stimuli in humans and monkeys. One of the most well-characterized components of this neural response, the P300 component of the event-related potential (ERP), is thought to represent the conscious processing, or encoding, of such stimuli (Soltani and Knight, 2000; Polich, 2007). The MTL-P300, recorded via depth electrodes in humans, is a locally generated version of the P300 associated with the hippocampal contribution (Halgren et al., 1998; Fell et al., 2004). Figure 6A depicts the average stimulus-evoked LFP aligned to stimulus onset for High Recognition and Low Recognition trials, averaged across all 114 LFPs. There was a significant divergence in the signal as early as 270 ms after stimulus onset that predicted subsequent recognition memory performance. We analyzed the magnitude of the stimulus-evoked LFP with respect to memory performance and attention throughout the session using a binning analysis, similar to our previous analysis for spike-field coherence. There was a significant positive relationship between LFP amplitude during stimulus encoding and subsequent recognition memory performance, as well as between LFP amplitude and looking time during encoding (Figure 6B–C). These data suggest that unlike gamma-band coherence, changes in the LFP amplitude reflect both attention and memory on a trial-by-trial basis, which is consistent with previous studies associating the P300 with attentional processing (Kok, 2001) and hippocampal-dependent processing of novel stimuli (Knight, 1996). Interestingly, this P300-like effect did not begin until nearly 170 ms after the earliest effects seen in gamma-band spike-field coherence.

Additional Behavioral Controls

We also considered the possibility that changes in behavior or neuronal activity through the recording session may affect the interpretation of these results. On average, the monkeys required 58 minutes to complete the session, viewing two presentations of each of 200 stimuli. It is possible that the stimuli presented at the beginning and end of the session evoked different neuronal responses. It is also possible that the monkey experienced fatigue through the session that influenced his performance. To address this issue, we analyzed memory performance, stimulus-evoked firing rates, and the magnitude of SFC with respect to time within the recording session. One-way ANOVAs revealed that there was no significant relationship between time within the session and recognition memory ($F_{(9,439)}=0.57$, $p>0.1$; Figure 7), absolute looking time during novel stimulus presentation ($F_{(9,437)}=0.39$, $p>0.1$; Figure 7A), firing rate modulation ($F_{(9,850)}=0.28$, $p>0.1$; Figure 7B), or gamma-band SFC ($F_{(9,1740)}=0.96$, $p>0.1$; Figure 7C). However, there was a significant negative correlation between LFP amplitude and the time course of the recording session ($F_{(9,1120)}=2.22$, $p<0.05$; Figure 7D).

Because this was the only measure which showed any significant correlation with time within the session, it is unclear whether this decline in LFP amplitude is related to fatigue, or some other mechanism.

Additionally, we determined the amount of time required to achieve fixation before each stimulus presentation. An increased time to achieve fixation would indicate that the monkey's attention or arousal level had declined. Over all 45 recording sessions, we found that that there was no significant difference in this measure between High Recognition and Low Recognition trials ($p > 0.10$). These data suggest that fluctuations in general alertness or arousal levels are not correlated with modulations in gamma-band synchronization in the hippocampus.

Discussion

Our findings show that spikes from isolated single units in the hippocampus are phase locked to each other and to gamma-band oscillations in simultaneously recorded hippocampal LFPs during memory encoding. Further, the magnitude of this phase locking is correlated with subsequent recognition memory performance. These results suggest that memory encoding is accompanied by enhanced coordination between hippocampal neurons.

Fell and colleagues previously showed that successful recognition memory encoding is correlated with increased gamma-band synchronization between local EEG oscillations in the hippocampus and rhinal cortex of human epilepsy patients (Fell et al., 2001). The current findings extend these observations to hippocampal neurons, indicating that single units within the hippocampus synchronize the timing of their spikes to the local network oscillations during memory formation, perhaps as a mechanism by which neurons sharing similar response properties might undergo functional coupling. We also found that gamma-band power in hippocampal LFPs during encoding is significantly correlated with subsequent recognition memory performance. These results are consistent with studies in human epileptic patients that have associated changes in hippocampal gamma-band oscillations with memory (Sederberg et al., 2007a; Sederberg et al., 2007b). Similar observations have been made in monkey parietal cortex in relation to working memory (Pesaran et al., 2002). In that study, both power and coherence in the gamma band were elevated during the delay period of a working memory task. Taken together, these findings suggest that synchronization between spiking activity and oscillatory field activity may be an important mechanism for holding a representation of behaviorally relevant stimuli "on-line".

Previous studies in rodents have linked hippocampal gamma-band synchronization to memory processes (Robbe et al., 2006; Montgomery and Buzsaki, 2007). In these studies, both the power and the coherence of gamma-band oscillations in hippocampal LFPs were enhanced in relation to the cognitive demands of a hippocampal-dependent task. Consistent with the current study, it was shown that modulations in neuronal synchronization can be dissociated from modulations in firing rate (Robbe et al., 2006), further supporting the notion that changes in the temporal structure of neuronal activity may affect computational outcomes. The current study extends these findings by showing a direct relationship between hippocampal gamma-band coherence and recognition memory performance.

How might gamma-band synchronization in the hippocampus improve encoding? By ensuring that the activity of multiple neurons is correlated within short (i.e., 10 ms) temporal windows, gamma-band synchronization could underlie the transient formation of functional neuronal ensembles (Fries, 2005; Womelsdorf et al., 2007). For example, a population of neurons may respond to a particular stimulus by synchronizing its firing in the gamma range, and this may contribute spike timing-dependent long-term potentiation (Bi and Poo, 1998), thereby strengthening the connections between these neurons. Gamma-band synchronization among

hippocampal neurons may also serve to enhance the impact of hippocampal neurons on output targets in the entorhinal cortex. For example, gamma-band synchronization may result in increased temporal summation of synaptic input on neurons downstream of hippocampal ensembles, thereby increasing the likelihood that these neurons will fire. Such a mechanism would in turn enhance the relay of memory signals to higher-order sensory areas and other areas important for memory storage. Although the difference in average coherence measures between recognition memory conditions is small, evidence from computational studies suggests that small increases in even weakly correlated inputs to neurons can cause substantial increases in the probability of firing of downstream neurons (Salinas and Sejnowski, 2000).

One caveat is that spike-field coherence does not directly reflect synchronization in the signals being projected to downstream areas, but only implies such an interaction, assuming that some component of the output is reflected in the LFP. Although the results of our analysis of spike-spike coherence provide evidence for synchrony among hippocampal units, future studies are needed to provide a more direct measurement of the degree to which synchronization within the hippocampus affects changes in the activity of downstream targets, e.g. with simultaneous recordings in the hippocampus and the entorhinal cortex.

It is important to consider the extent to which memory effects can be dissociated from attentional effects in assessing performance on the VPLT. Although these processes cannot be completely dissociated with this behavioral task, there is evidence from previous studies that memory and attention depend on different brain regions. In particular, the finding that monkeys with hippocampal lesions (Zola et al., 2000) and amnesic patients (McKee and Squire, 1993) display intact novelty preference as long as the delay between first and second stimulus presentation is short (1 second, and 0.5 seconds, respectively) but are impaired with increasing delays (10 seconds and longer) supports this idea. At the same time, increased attention during stimulus presentation may lead to better subsequent memory. This could result in neural signals that underlie both processes co-varying with behavioral performance. Our data suggest that gamma-band coherence in the hippocampus more reliably predicts successful recognition memory performance than increased attention to stimuli. In contrast, the stimulus-evoked LFP in the hippocampus appears to reflect both memory encoding and attentional processes.

To our knowledge, this study is unique in its separation of gamma-band oscillations recorded in the primate hippocampus into high and low gamma. A number of recent studies have observed oscillatory synchrony in either high or low gamma in other brain regions, and in many cases these frequency bands have been associated with distinct aspects of cognition (Edwards et al., 2005; Hoogenboom et al., 2006; Wyart and Tallon-Baudry, 2008, 2009). Cortical oscillations in the high gamma band tend to exhibit higher phase-locking with theta oscillations in humans (Canolty et al., 2006) and rodents (Sirota et al., 2008). Additionally, oscillations in the high gamma-band range have been associated with the hemodynamic response measured using BOLD fMRI (Niessing et al., 2005).

In the current study, the results of the non-parametric test for single units revealed a significant difference across memory conditions only for the high gamma neurons. However, analyses including both high and low gamma neurons revealed significant differences between successful (high recognition) and less successful (low recognition) encoding (Figure 3C), as well as a significant positive correlation between trial-by-trial modulations in coherence and recognition memory (Figure 4). Nevertheless, these different populations of neurons may make distinct contributions to behavior through their participation in different modes of network activity.

Visual stimuli induced a clear increase in gamma-band synchronization that was associated with recognition memory performance. However, we also observed some gamma-band

synchronization prior to stimulus onset. Non-parametric randomization tests applied to the pre-stimulus period revealed that neither gamma-band coherence nor power was correlated with subsequent recognition memory performance during this period (Supplemental Figures 2, 3, 5 and 6), suggesting that the observed level of pre-stimulus synchronization reflects hippocampal processing unrelated to the behavioral task. One possibility is that this pre-stimulus synchronization reflects arousal mechanisms. Timing was held constant throughout the experiment (1 second fixation period), so it would be possible for the monkeys to anticipate the onset of the stimulus. Alternatively, between the end of the previous stimulus presentation and the beginning of the next the monkey may be engaged in retrieving previous stimuli, encoding new information, or some other uncontrolled process. Because some hippocampal function is likely during such processes, the presence of spike-field coherence during this interval is not wholly surprising. Functional imaging studies often employ a separate task during baseline periods because the use of a simple "rest" period can potentially lead to high levels of hippocampal activation (Stark and Squire, 2001).

While several studies have identified activity at the cellular level related to recognition memory in the cortex surrounding the hippocampus (Miller et al., 1991; Riches et al., 1991; Miller et al., 1993; Sobotka and Ringo, 1993; Suzuki et al., 1997), there is a notable lack of evidence for recognition memory signals in the hippocampus proper. One important difference between our task and those used in previous neurophysiological studies is the degree of training involved. The VPLT requires only simple fixation training. In contrast, the tasks used in previous neurophysiology studies require a long period of training (up to 7–10 months), during which monkeys gradually learn a match-to-sample rule. It is conceivable that during this training period, monkeys acquire strategies for performing the task that do not rely on the hippocampus. Similarly, while the VPLT examines the monkey's innate preference for novelty, tasks in previous studies examined the monkey's ability to respond correctly in order to receive a food or juice reward. The reward component of these tasks may encourage the acquisition of strategies that recruit extra-hippocampal structures. Consistent with this idea, the VPLT has been shown to be more sensitive than the delayed non-matching to sample task to restricted lesions of the hippocampus (Pascalis and Bachevalier, 1999; Zola et al., 2000; Nemanic et al., 2004).

In summary, we have utilized spectral analysis to examine the role of precise spike timing in the hippocampus in memory formation. Our results are consistent with the idea that memory encoding in the medial temporal lobe relies on a combination of firing rate changes at the single-cell level, and altered patterns of synchronization at the population level.

Supplementary Material

Refer to Web version on PubMed Central for supplementary material.

Acknowledgments

We thank E. Stanley and M. Tompkins for technical assistance, and R. D. Burwell, R. Desimone, J. R. Manns, and L. R. Squire for comments on the manuscript. This research was supported by the Yerkes National Primate Research Center through base grant RR00165 from the National Institutes of Health, Ernst-Strüngmann-Institute Ltd., Emory Alzheimer's Disease Research Center grant AG025688 (E.A.B.), the NIGMS (M.J.J.), and grants from the National Institute of Mental Health, MH080007 (E.A.B.) and MH082559 (M.J.J.).

References

Baxter MG, Murray EA. Opposite relationship of hippocampal and rhinal cortex damage to delayed nonmatching-to-sample deficits in monkeys. Hippocampus 2001a;11:61–71. [PubMed: 11261774]

Baxter MG, Murray EA. Effects of hippocampal lesions on delayed nonmatching-to-sample in monkeys: A reply to Zola and Squire (2001). Hippocampus 2001b;11:201–203. [PubMed: 11769304]

Bi GQ, Poo MM. Synaptic modifications in cultured hippocampal neurons: dependence on spike timing, synaptic strength, and postsynaptic cell type. J Neurosci 1998;18:10464–10472. [PubMed: 9852584]

Bichot NP, Rossi AF, Desimone R. Parallel and serial neural mechanisms for visual search in macaque area V4. Science 2005;308:529–534. [PubMed: 15845848]

Bragin A, Jando G, Nadasdy Z, Hetke J, Wise K, Buzsaki G. Gamma (40–100 Hz) oscillation in the hippocampus of the behaving rat. J Neurosci 1995;15:47–60. [PubMed: 7823151]

Brown MW, Wilson FAW, Riches IP. Neuronal evidence that inferomedial temporal cortex is more important than hippocampus in certain processes underlying recognition memory. Brain Res 1987;409:158–162. [PubMed: 3107754]

Buschman TJ, Miller EK. Top-Down Versus Bottom-Up Control of Attention in the Prefrontal and Posterior Parietal Cortices. Science 2007;315:1860–1862. [PubMed: 17395832]

Buzsaki G. Large-scale recording of neuronal ensembles. Nat Neurosci 2004;7:446–451. [PubMed: 15114356]

Canolty RT, Edwards E, Dalal SS, Soltani M, Nagarajan SS, Kirsch HE, Berger MS, Barbaro NM, Knight RT. High gamma power Is phase-locked to theta oscillations in human neocortex. Science 2006;313:1626–1628. [PubMed: 16973878]

Chrobak JJ, Buzsaki G. High-frequency oscillations in the output networks of the hippocampal-entorhinal axis of the freely behaving rat. J Neurosci 1996;16:3056–3066. [PubMed: 8622135]

Csicsvari J, Jamieson B, Wise KD, Buzsaki G. Mechanisms of gamma oscillations in the hippocampus of the behaving rat. Neuron 2003;37:311–322. [PubMed: 12546825]

Edwards E, Soltani M, Deouell LY, Berger MS, Knight RT. High Gamma Activity in Response to Deviant Auditory Stimuli Recorded Directly From Human Cortex. J Neurophysiol 2005;94:4269–4280. [PubMed: 16093343]

Fell J, Klaver P, Lehnertz K, Grunwald T, Schaller C, Elger CE, Fernandez G. Human memory formation is accompanied by rhinal-hippocampal coupling and decoupling. Nat Neurosci 2001;4:1259–1264. [PubMed: 11694886]

Fell J, Dietl T, Grunwald T, Kurthen M, Klaver P, Trautner P, Schaller C, Elger CE, Fernandez G. Neural bases of cognitive ERPs: more than phase reset. J Cogn Neurosci 2004;16:1595–1604. [PubMed: 15601521]

Fries P, Reynolds JH, Rorie AE, Desimone R. Modulation of oscillatory neuronal synchronization by selective visual attention. Science 2001;291:1560–1563. [PubMed: 11222864]

Fries P, Womelsdorf T, Oostenveld R, Desimone R. The effects of visual stimulation and selective visual attention on rhythmic neuronal synchronization in macaque area V4. J Neurosci 2008;28:4823–4835. [PubMed: 18448659]

Halgren E, Marinkovic K, Chauvel P. Generators of the late cognitive potentials in auditory and visual oddball tasks. Electroencephalogr Clin Neurophysiol 1998;106:156–164. [PubMed: 9741777]

Hoogenboom N, Schoffelen J-M, Oostenveld R, Parkes LM, Fries P. Localizing human visual gamma-band activity in frequency, time and space. Neuroimage 2006;29:764–773. [PubMed: 16216533]

Jarvis MR, Mitra PP. Sampling properties of the spectrum and coherency of sequences of action potentials. Neural Comput 2001;13:717–749. [PubMed: 11255566]

Kilner JM, Baker SN, Salenius S, Hari R, Lemon RN. Human cortical muscle coherence is directly related to specific motor parameters. J Neurosci 2000;20:8838–8845. [PubMed: 11102492]

Knight R. Contribution of human hippocampal region to novelty detection. Nature 1996;383:256–259. [PubMed: 8805701]

Kok A. On the utility of P3 amplitude as a measure of processing capacity. Psychophysiology 2001;38:557–577. [PubMed: 11352145]

Manns JR, Hopkins RO, Reed JM, Kitchener EG, Squire LR. Recognition memory and the human hippocampus. Neuron 2003;37:171–180. [PubMed: 12526782]

Maris E, Oostenveld R. Nonparametric statistical testing of EEG- and MEG-data. J Neurosci Methods 2007;164:177–190. [PubMed: 17517438]

Markram H, Lubke J, Frotscher M, Sakmann B. Regulation of synaptic efficacy by coincidence of postsynaptic APs and EPSPs. Science 1997;275:213–215. [PubMed: 8985014]

McKee RD, Squire LR. On the development of declarative memory. J Exp Psychol Learn Mem Cogn 1993;19:397–404. [PubMed: 8454964]

Miller EK, Li L, Desimone R. A neural mechanism for working and recognition memory in inferior temporal cortex. Science 1991;254:1377–1379. [PubMed: 1962197]

Miller EK, Li L, Desimone R. Activity of neurons in anterior inferior temporal cortex during a short-term memory task. J Neurosci 1993;13:1460. [PubMed: 8463829]

Mishra J, Fellous JM, Sejnowski TJ. Selective attention through phase relationship of excitatory and inhibitory input synchrony in a model cortical neuron. Neural Netw 2006;19:1329–1346. [PubMed: 17027225]

Mitra PP, Pesaran B. Analysis of dynamic brain imaging data. Biophys J 1999;76:691–708. [PubMed: 9929474]

Montgomery SM, Buzsaki G. Gamma oscillations dynamically couple hippocampal CA3 and CA1 regions during memory task performance. Proc Natl Acad Sci U S A 2007;104:14495–14500. [PubMed: 17726109]

Murray EA, Mishkin M. Object Recognition and Location Memory in Monkeys with Excitotoxic Lesions of the Amygdala and Hippocampus. J Neurosci 1998;18:6568–6582. [PubMed: 9698344]

Nemanic S, Alvarado MC, Bachevalier J. The hippocampal/parahippocampal regions and recognition memory: insights from visual paired comparison versus object-delayed nonmatching in monkeys. J Neurosci 2004;24:2013–2026. [PubMed: 14985444]

Nichols TE, Holmes AP. Nonparametric permutation tests for functional neuroimaging: A primer with examples. Hum Brain Mapp 2002;15:1–25. [PubMed: 11747097]

Niessing J, Ebisch B, Schmidt KE, Niessing M, Singer W, Galuske RAW. Hemodynamic Signals Correlate Tightly with Synchronized Gamma Oscillations. Science 2005;309:948–951. [PubMed: 16081740]

Pascalis O, Bachevalier J. Neonatal aspiration lesions of the hippocampal formation impair visual recognition memory when assessed by paired-comparison task but not by delayed nonmatching-to-sample task. Hippocampus 1999;9:609–616. [PubMed: 10641753]

Pesaran B, Pezaris JS, Sahani M, Mitra PP, Andersen RA. Temporal structure in neuronal activity during working memory in macaque parietal cortex. Nat Neurosci 2002;5:805–811. [PubMed: 12134152]

Polich J. Updating P300: an integrative theory of P3a and P3b. Clin Neurophysiol 2007;118:2128–2148. [PubMed: 17573239]

Riches IP, Wilson FAW, Brown MW. The effects of visual stimulation and memory on neurons of the hippocampal formation and the neighboring parahippocampal gyrus and inferior temporal cortex of the primate. J Neurosci 1991;11:1763–1779. [PubMed: 2045886]

Robbe D, Montgomery SM, Thome A, Rueda-Orozco PE, McNaughton BL, Buzsaki G. Cannabinoids reveal importance of spike timing coordination in hippocampal function. Nat Neurosci 2006;9:1526–1533. [PubMed: 17115043]

Rolls ET, Cahusac PMB, Feigenbaum JD, Miyashita Y. Responses of single neurons in the hippocampus of the macaque related to recognition memory. Exp Brain Res 1993;93:299–306. [PubMed: 8491268]

Rolls ET, Miyashita Y, Cahusac PM, Kesner RP, Niki H, Feigenbaum JD, Bach L. Hippocampal neurons in the monkey with activity related to the place in which a stimulus is shown. J Neurosci 1989;9:1835–1845. [PubMed: 2723752]

Rosenberg JR, Amjad AM, Breeze P, Brillinger DR, Halliday DM. The Fourier approach to the identification of functional coupling between neuronal spike trains. Prog Biophys Mol Biol 1989;53:1–31. [PubMed: 2682781]

Rutishauser U, Mamelak AN, Schuman EM. Single-trial learning of novel stimuli by individual neurons of the human hippocampus-amygdala complex. Neuron 2006;49:805–813. [PubMed: 16543129]

Salinas E, Sejnowski TJ. Impact of correlated synaptic input on output firing rate and variability in simple neuronal models. J Neurosci 2000;20:6193–6209. [PubMed: 10934269]

Sederberg PB, Schulze-Bonhage A, Madsen JR, Bromfield EB, Litt B, Brandt A, Kahana MJ. Gamma oscillations distinguish true from false memories. Psychol Sci 2007a;18:927–932. [PubMed: 17958703]

Sederberg PB, Schulze-Bonhage A, Madsen JR, Bromfield EB, McCarthy DC, Brandt A, Tully MS, Kahana MJ. Hippocampal and neocortical gamma oscillations predict memory formation in humans. Cereb Cortex 2007b;17:1190–1196. [PubMed: 16831858]

Sirota A, Montgomery S, Fujisawa S, Isomura Y, Zugaro M, Buzsaki G. Entrainment of neocortical neurons and gamma oscillations by the hippocampal theta rhythm. Neuron 2008;60:683–697. [PubMed: 19038224]

Sobotka S, Ringo JL. Investigation of long-term recognition and association memory in unit responses from inferotemporal cortex. Exp Brain Res 1993;96:28–38. [PubMed: 8243581]

Soltani M, Knight RT. Neural origins of the P300. Crit Rev Neurobiol 2000;14:199–224. [PubMed: 12645958]

Stark CE, Squire LR. When zero is not zero: the problem of ambiguous baseline conditions in fMRI. Proc Natl Acad Sci U S A 2001;98:12760–12766. [PubMed: 11592989]

Suzuki WA, Miller EK, Desimone R. Object and place memory in the macaque entorhinal cortex. J Neurophysiol 1997;78:1062–1081. [PubMed: 9307135]

Taylor K, Mandon S, Freiwald WA, Kreiter AK. Coherent oscillatory activity in monkey area V4 predicts successful allocation of attention. Cereb Cortex 2005;15:1424–1437. [PubMed: 15659657]

Wilson FAW, Goldman-Rakic PS. Viewing preferences of rhesus monkeys related to memory for complex pictures, colours and faces. Behav Brain Res 1994;60:79–89. [PubMed: 8185855]

Womelsdorf T, Fries P, Mitra PP, Desimone R. Gamma-band synchronization in visual cortex predicts speed of change detection. Nature 2006;439:733–736. [PubMed: 16372022]

Womelsdorf T, Schoffelen J-M, Oostenveld R, Singer W, Desimone R, Engel AK, Fries P. Modulation of neuronal interactions through neuronal synchronization. Science 2007;316:1609–1612. [PubMed: 17569862]

Wyart V, Tallon-Baudry C. Neural dissociation between visual awareness and spatial attention. J Neurosci 2008;28:2667–2679. [PubMed: 18322110]

Wyart V, Tallon-Baudry C. How ongoing fluctuations in human visual cortex predict perceptual awareness: baseline shift versus decision bias. J Neurosci 2009;29:8715–8725. [PubMed: 19587278]

Xiang JZ, Brown MW. Differential neuronal encoding of novelty, familiarity and recency in regions of the anterior temporal lobe. Neuropharmacology 1998;37:657–676. [PubMed: 9705004]

Zeitler M, Fries P, Gielen S. Assessing Neuronal Coherence with Single-Unit, Multi-Unit, and Local Field Potentials. Neural Comput 2006;18:2256–2281. [PubMed: 16846392]

Zola SM, Squire LR. Relationship between magnitude of damage to the hippocampus and impaired recognition memory in monkeys. Hippocampus 2001;11:92–98. [PubMed: 11345130]

Zola SM, Squire LR, Teng E, Stefanacci L, Buffalo EA, Clark RE. Impaired recognition memory in monkeys after damage limited to the hippocampal region. J Neurosci 2000;20:451–463. [PubMed: 10627621]

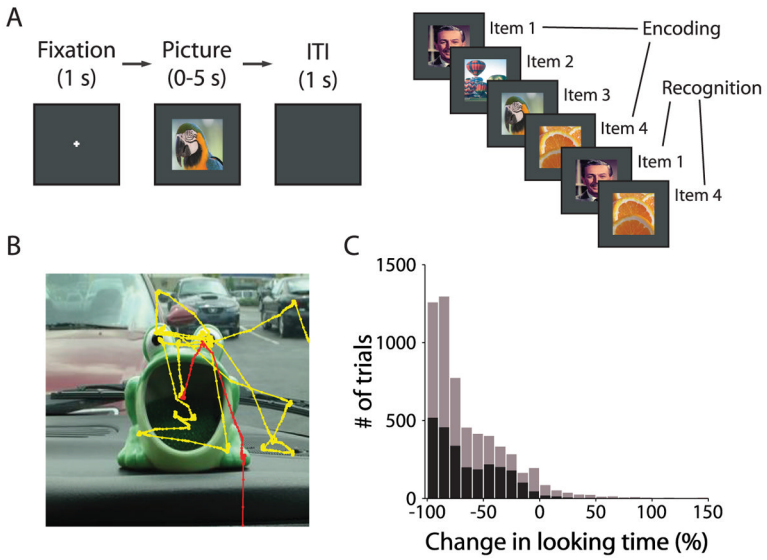

Fig. 1. Behavioral Task and Performance

(A) VPLT design. Two-hundred unique stimuli were presented in each test session, with up to 8 trials intervening between the first and second presentations. Each trial began with a required 1 second fixation period and trials were separated by a 1 second inter-trial interval. (B) An example of the monkey's scan path over the first (yellow) and second (red) presentations of a stimulus. The monkey spent much less time viewing the stimulus in the second presentation. (C) Combined behavioral data from 45 test sessions in two monkeys. The histogram depicts the change in looking time for each stimulus as a percentage of the amount of time the monkey spent looking at the first presentation of each stimulus (black: Monkey A; gray: Monkey B). A negative change represents stimuli for which looking times were longer during the first presentation. For clarity, trials with a percent change in looking time of greater than 150% are not shown (these represented a total of 5 trials, or 0.2 trials per session, for Monkey A and 22 trials, or 1.1 trials per session, for Monkey B).

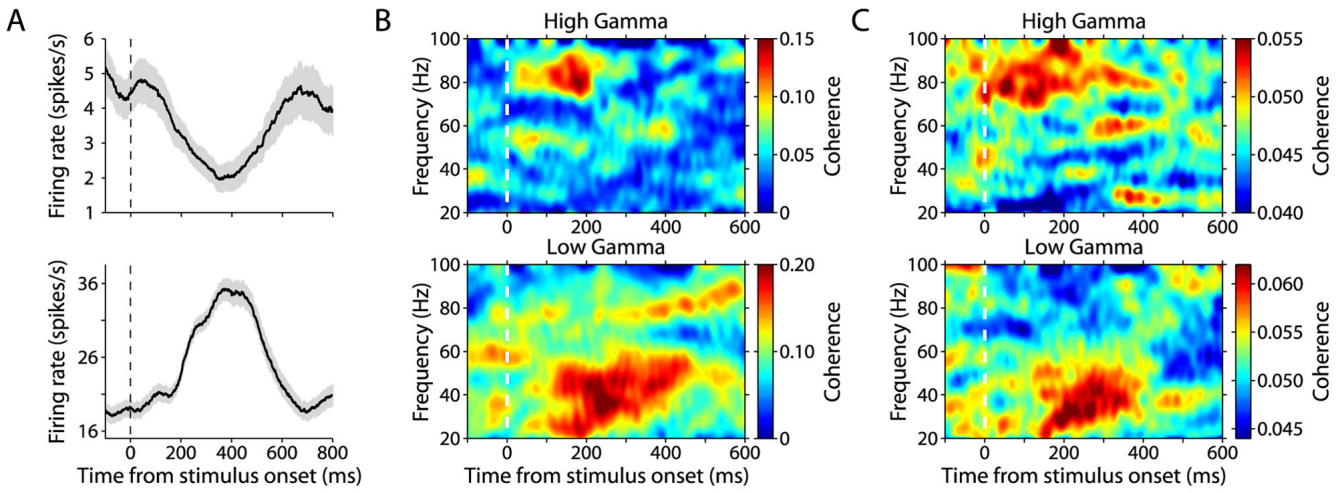

Fig. 2. Firing Rate and Spike-Field Coherence During Stimulus Encoding

(A) Average firing rates for two example hippocampal neurons during encoding. Shaded areas represent SEM. (B) Spike-field coherence as a function of time (X-Axis) and frequency (Y-Axis) during all encoding trials for the two example neurons shown in (A); coherence was calculated between the neuron on one electrode and the LFP recorded on a separate electrode. (C) Coherence as a function of time and frequency averaged across all encoding trials for high gamma (top) and low gamma (bottom) neurons.

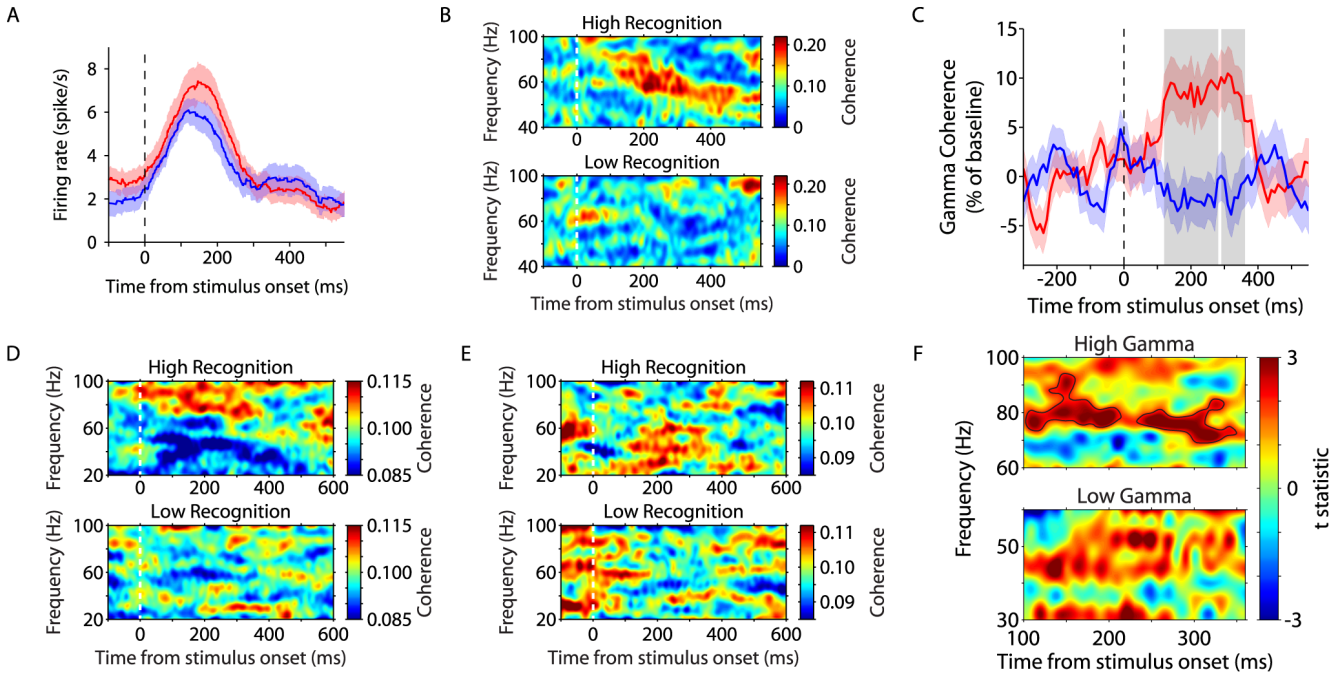

Fig. 3. Gamma-band Spike-field Coherence During Stimulus Encoding Predicts Subsequent Recognition

(A) Average firing rate of an example hippocampal neuron for high recognition (red) and low recognition (blue) trials. There was no difference in firing rate across conditions. Red and blue shaded areas represent SEM. (B) Coherence as a function of time and frequency between the example neuron in (A) and the LFP recorded on a separate electrode, for high recognition (top) and low recognition (bottom) trials. Coherence (52–68 Hz) was significantly enhanced during the encoding of subsequently well-recognized stimuli. (C) Gamma-band coherence expressed as percentage of baseline averaged over 175 hippocampal recording pairs, during high recognition (red) and low recognition (blue) trials, as a function of time from stimulus onset. Red and blue shaded areas represent SEM. Gray shaded area represents time points at which gamma-band coherence was significantly different for the two conditions ($p < 0.01$). (D) Coherence averaged across all high gamma neurons, for high recognition (top) and low recognition (bottom) trials. (E) Same as (D), but for low gamma neurons. (F) Modulation of coherence between high recognition and low recognition trials, for high gamma (top) and low gamma (bottom). Areas of significant coherence modulation are outlined in black (non-parametric randomization test, corrected for multiple comparisons across time and frequency).

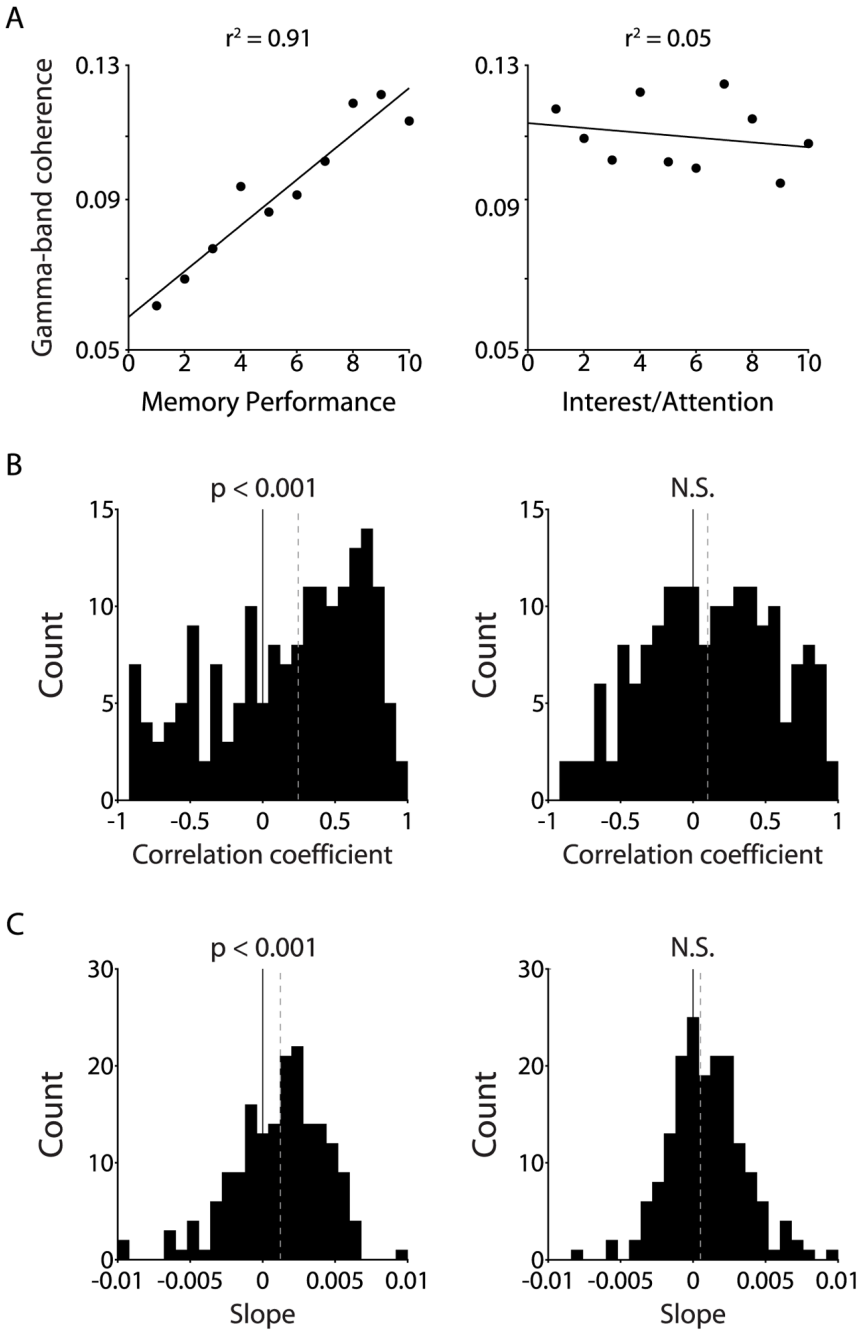

Fig. 4. Coherence is Correlated with Recognition Memory, but not with Attention

(A) Gamma-band spike-field coherence for one example neuron-LFP pair, binned according to percent change in looking time (left) or looking time during encoding (right). Line indicates linear fit to data. (B) Histograms depicting correlation coefficients between gamma-band spike-field coherence and behavior across all neuron-LFP pairs when binned according to percent change in looking time (left) or looking time during encoding (right). Black line indicates zero; dashed gray line indicates median. (C) Same as (B), but for slopes. Dashed gray line indicates median.

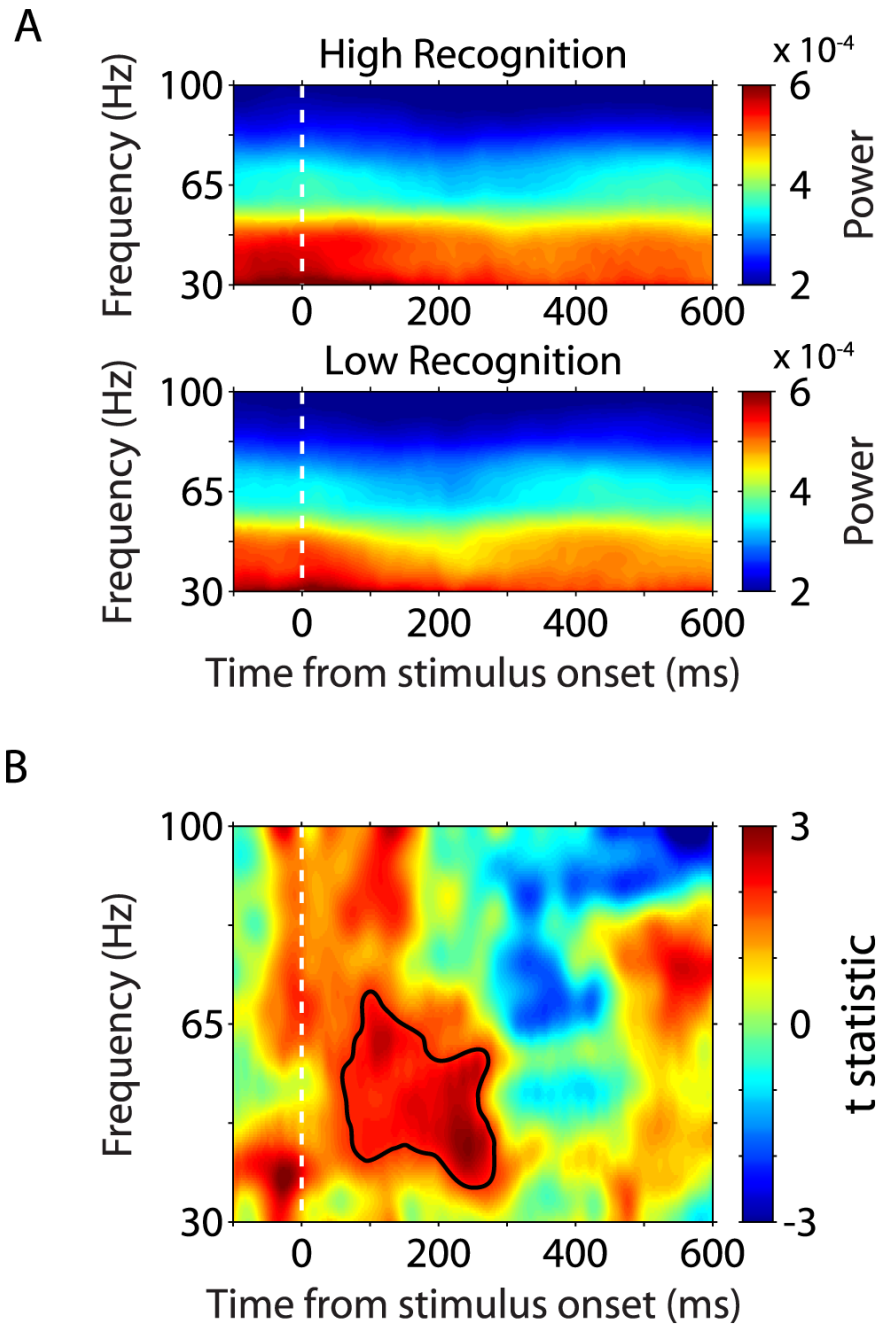

Fig. 5. Gamma-band LFP Power During Stimulus Encoding Predicts Subsequent Recognition

(A) Gamma-band power averaged across all LFPs during the encoding of high recognition (top) and low recognition (bottom) stimuli. LFP spectra have been normalized by $1/f$ for visualization. (B) Modulation of gamma-band power between high recognition and low recognition stimuli. The area of significant power modulation is outlined in black (non-parametric randomization test, corrected for multiple comparisons across time and frequency).

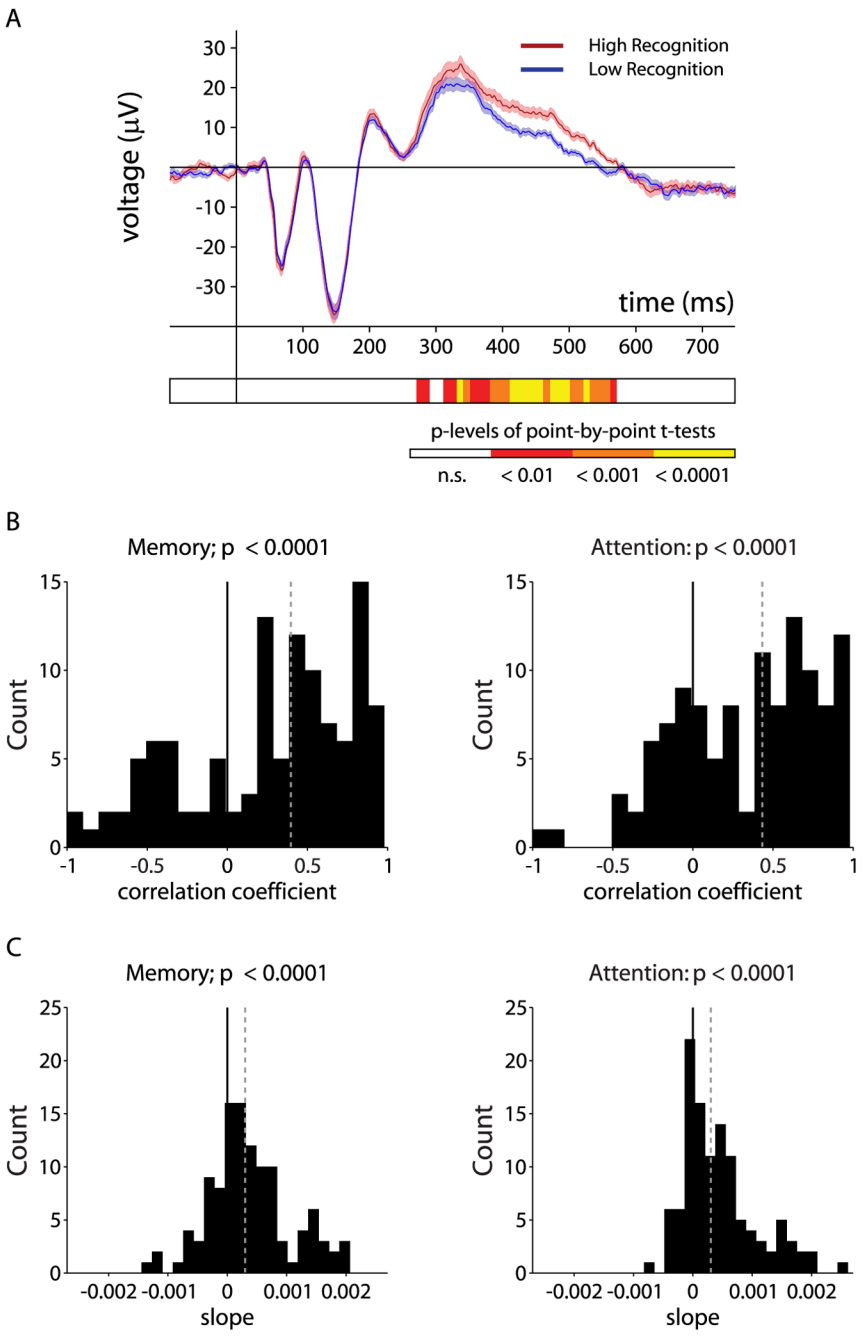

Fig. 6. Stimulus-evoked LFP is Modulated by both Attention and Recognition Memory

(A) Stimulus-evoked modulations in LFP amplitude averaged across 114 LFPs during encoding of High Recognition (red) and Low Recognition (blue) stimuli. Shaded areas represent standard error of the mean. *P*-values for significance tests at each consecutive 10 ms time-bin are shown in the color plot below the graph. Time bins shown in yellow represent *p*-values less than 0.0001. (B) Histograms depicting correlation coefficients of the linear functions fit to LFP data across all LFPs when binned according to percent change in looking time (left) or looking time during encoding (right). Black line indicates zero; dashed gray line indicates median. (C) Same as (B), but for slopes. Dashed gray line indicates median.

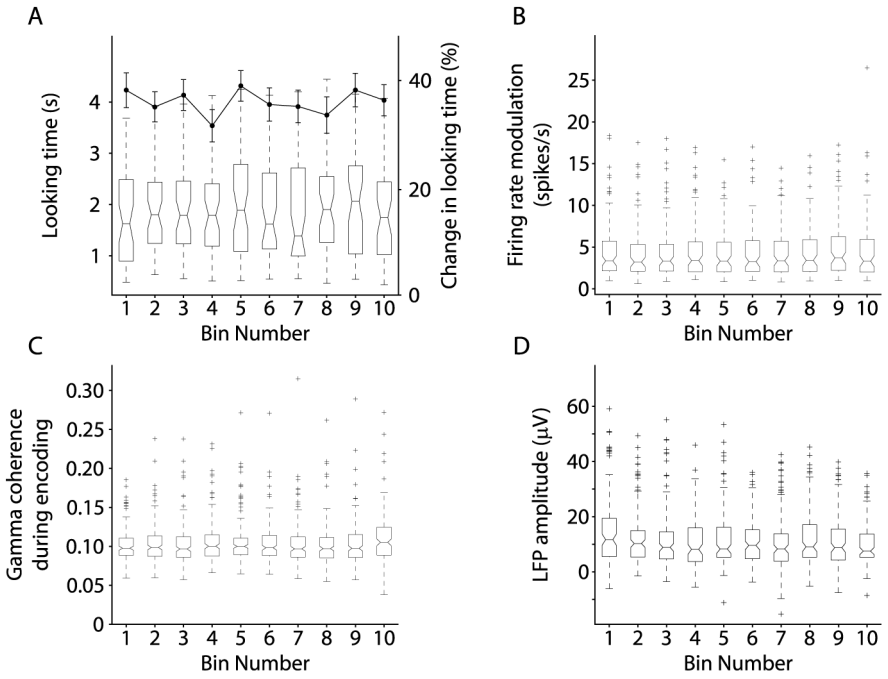

Fig. 7. Behavioral and Neural Measures as a Function of Time within Session

(A) Box plot: Absolute looking time during novel stimulus presentation, averaged within bins of 20 trials each, across recording sessions. There was no significant effect of bin number on looking time. Line plot: percent change in looking time averaged within bins of 20 trials each, across all recording sessions. There was no significant effect of bin number on behavior across sessions. (B) Magnitude of the response for all visually responsive neurons, averaged within bins of 20 trials each, across recording sessions. There was no significant effect of bin number on firing rate across neurons. (C) Gamma-band spike-field coherence for all visually responsive neurons, averaged within each bin, across recording sessions. There was no significant effect of bin number on coherence across neuron-LFP pairs. (D) LFP amplitude across the 270–570 ms period after novel stimulus onset for all LFPs, averaged within each bin, across recording sessions. There was a significant negative correlation between LFP amplitude and the time course of the recording session (One-way ANOVA, $F_{(9,1120)}=2.22$, $p<0.05$).